

PCCP

Accepted Manuscript



This is an *Accepted Manuscript*, which has been through the Royal Society of Chemistry peer review process and has been accepted for publication.

Accepted Manuscripts are published online shortly after acceptance, before technical editing, formatting and proof reading. Using this free service, authors can make their results available to the community, in citable form, before we publish the edited article. We will replace this *Accepted Manuscript* with the edited and formatted *Advance Article* as soon as it is available.

You can find more information about *Accepted Manuscripts* in the [Information for Authors](#).

Please note that technical editing may introduce minor changes to the text and/or graphics, which may alter content. The journal's standard [Terms & Conditions](#) and the [Ethical guidelines](#) still apply. In no event shall the Royal Society of Chemistry be held responsible for any errors or omissions in this *Accepted Manuscript* or any consequences arising from the use of any information it contains.

Topology of the magnetically induced current density and proton magnetic shielding in hydrogen bonded systems[†]

Guglielmo Monaco,^a Paolo Della Porta,^a Mirosław Jabłoński,^b and Riccardo Zanasi^{*a}

Received Xth XXXXXXXXXXXX 20XX, Accepted Xth XXXXXXXXXXXX 20XX

First published on the web Xth XXXXXXXXXXXX 200X

DOI: 10.1039/b000000x

It is pointed out that a common feature of the current density induced in hydrogen bonded systems X–H···Y–Z by a magnetic field perpendicular to the H-bond is a continuous stagnation line made of (2,0) saddle points. The saddle line cuts the H-bond almost perpendicularly near the bond critical point (BCP). This implies the confinement of the current density within three basins of current delimited by two separatrices formed by all the asymptotic trajectories originating and terminating at the saddle points. Then, the perpendicular nuclear magnetic shielding (and magnetizability) are partitioned in three contributions: one for the X–H fragment, one for Y–Z, and an external one surrounding the former two. This permits to ascertain that the largely decreased perpendicular proton magnetic shielding is determined by a local effect inside the X–H domain due, ultimately, to a minimal loss of electron charge density around the hydrogen. A drop as small as 2–3% of an electron within a restricted region around the hydrogen nucleus causes a deshielding effect as large as 4.5–5 ppm, namely 20% of the free-molecule shielding, thus making NMR a very sensitive technique for detecting hydrogen bond formation, as it is well-known experimentally.

1 Introduction

An updated definition of the hydrogen bond has been recently presented by the International Union of Pure and Applied Chemistry (IUPAC) Task Group #2004-026-2-100.¹ The definition is a short one, followed by a list of experimental and theoretical criteria and footnotes that can be used to assess the presence of the hydrogen bond.^{2,3} Though the updated definition provides a necessary improvement over the previous one, as contained in the IUPAC Compendium of Chemical Terminology (informally known as the Gold Book⁴), apparently no strong agreement has been found yet. Indeed, on the one hand, soon after the IUPAC recommendations, Weinhold and Klein have proposed a one-statement definition of hydrogen bond that incorporates the majority of experimental and theoretical observations;⁵ on the other hand, the generality of the individual criteria is still under scrutiny.⁶ One of the most trusted among them is the experimental criterion (E5) of the IUPAC recommendations, which reads: “the X–H···Y–Z hydrogen bond leads to characteristic NMR signatures that typically include pronounced proton deshielding for H in X–H

...”.² Thus, the down-field shift of the proton magnetic resonance is considered one of the best evidences for hydrogen bond formation and is recognized to be a direct consequence of the electron redistribution around the H atom following the formation of the bond. Actually, for families of similar substances, a few excellent linear relationships between proton NMR chemical shift and hydrogen bond strength have been determined theoretically.^{7,8}

Advances in understanding the proton deshielding have been reported by McDowell and Buckingham⁹ studying linear Cl–H···Y–Z complexes. They found that the hydrogen bond formation increases the proton nuclear magnetic shielding parallel to the H-bond (σ_{\parallel}^H) and largely decreases the perpendicular components (σ_{\perp}^H). As a result, the isotropic proton shielding constant ($\sigma_{\text{iso}}^H = \frac{1}{3}\sigma_{\parallel}^H + \frac{2}{3}\sigma_{\perp}^H$) becomes smaller, whilst the tensor anisotropy ($\sigma_{\text{aniso}}^H = \sigma_{\parallel}^H - \sigma_{\perp}^H$) becomes larger on H-bond formation. Indeed, for a series of X–H···O complexes the isotropic and anisotropic shielding constants of the proton engaged in a hydrogen bond have been found to correlate with the binding energy.¹⁰

The nuclear magnetic shielding can be defined in terms of the current density tensor,¹¹ then a connection between the H-bond strength and the strength of the current induced by a unitary magnetic field somewhere in-between the two H-bonded subunits can be devised.¹² In linear complexes the current density induced by a magnetic field parallel to the H-bond forms a purely diatropic vortex, which elongates all over the X–H···Y system. Therefore, one can conceive that the closer

[†] Electronic Supplementary Information (ESI) available: separatrices of the current density induced by a magnetic field perpendicular to the H-bond and perpendicular proton magnetic shielding density function difference maps of all the complexes considered in the study. See DOI: 10.1039/b000000x/

^a Department of Chemistry and Biology, University of Salerno, via Giovanni Paolo II 132, 84084 Fisciano, Italy. Fax: +39 089 969603; Tel: +39 089 969590; E-mail: rzanasi@unisa.it

^b Department of Quantum Chemistry, Nicolaus Copernicus University, 7-Gagarina St., PL-87 100 Toruń, Poland.

X–H and Y, the greater the parallel proton nuclear magnetic shielding. When the magnetic field is perpendicular to the H-bond the picture is a little more complex. Indeed, the penetration of the two—in most of the cases—conrotating diatropic vortices, which enclose X–H and Y–Z respectively, and the electronic rearrangement occurring during the H-bond formation generate a resulting current density whose effects on proton shielding are not directly deducible. It might be argued that the magnetization in Y should provide a proton deshielding, but there are indications that this is not the leading term.⁹

Since the pronounced proton deshielding that identifies the presence of the hydrogen bond is determined by $\sigma_{\perp}^{\text{H}}$, a deeper understanding of the current density induced by a unitary magnetic field perpendicular to the H-bond is highly desirable. The aim of this work is to show some results that give a clear representation of the quantum mechanical, first-order, electronic current density vector field $\mathbf{J}^{\mathbf{B}} = \mathbf{J}^{\mathbf{B}}(\mathbf{r})$ generated at point \mathbf{r} by a static, unitary magnetic field of flux \mathbf{B} perpendicular to the hydrogen bond for a number of X–H \cdots Y–Z linear complexes. The study, based on the topological analysis of $\mathbf{J}^{\mathbf{B}}$,^{13–17} with particular emphasis to the H-bond region, has allowed introducing the breakdown of $\sigma_{\perp}^{\text{H}}$ in physically sound regional terms. Then, the interpretation of the latter has spurred us to compare the proton magnetic shielding density functions of the complexes with those of the parent isolated monomers.

2 Calculation Methods

The five linear dimers studied by McDowell and Buckingham⁹ plus the CIH \cdots NCH complex have been considered. According to their study, the two complexes that can be obtained combining the somewhat special FB molecule with CIH have the smaller and the largest proton deshielding in the set. Therefore, those two complexes nicely open and close a rather evenly sampled range of proton magnetic shielding responses, which is fine for our purposes. Correlation effects on our main target, i.e., the magnetic response of the systems, have been taken into account at the DFT level. The same level of accuracy has been kept also during the auxiliary geometry optimization step for coherence. Then, equilibrium geometries were fully optimized with the Gaussian 09 suite of programs¹⁸ at the DFT level, using the B97-2 functional¹⁹ and the aug-cc-pVTZ basis set.^{20,21} Current densities and related magnetic properties were computed with the CTOCD-DZ2 method^{22–26} at DFT level,^{27–29} using the SYSMO package³⁰ and adopting the same combination of functional and basis set used for optimizing the structures. The advantages of the CTOCD method for calculation of currents are well documented.³¹ As shown by Flaig and coworkers,³² benchmarking hydrogen and carbon NMR chemical shifts, the B97-2 functional provides accurate magnetic properties. Moreover, B97-2 molecular struc-

tures have been found to be comparable to those obtained using other quite popular functionals.¹⁹ The aug-cc-pVTZ basis set is large enough to partially compensate for the basis set superposition error (BSSE).³³

3 Results and discussion

Bond lengths, interaction energies and proton magnetic shielding for the B97-2/aug-cc-pVTZ optimized linear structures are reported in Table 1. The changes in the shielding from the free CIH molecule upon complexation,

$$\Delta\sigma_{\perp}^{\text{H}} = \sigma_{\perp}^{\text{H}} - \sigma_{\perp, \text{XH}}^{\text{H}}, \quad (1)$$

$$\Delta\sigma_{\parallel}^{\text{H}} = \sigma_{\parallel}^{\text{H}} - \sigma_{\parallel, \text{XH}}^{\text{H}}, \quad (2)$$

$$\Delta\sigma_{\text{iso}}^{\text{H}} = \sigma_{\text{iso}}^{\text{H}} - \sigma_{\text{iso}, \text{XH}}^{\text{H}}, \quad (3)$$

are also given. As can be observed the variation of the perpendicular proton magnetic shielding on H-bond formation is always negative, ranging from -0.56 ppm for the very weakly bounded CIH \cdots FB complex to the -6.38 ppm for the rather more stable CIH \cdots BF dimer. Conversely, the change in the parallel proton magnetic shielding is always positive and less sensitive to the sort of complex. The resulting change in the isotropic component is negative in agreement with criteria (E5) of the IUPAC recommendation,² with the only exception of the small positive $\Delta\sigma_{\text{iso}}^{\text{H}}$ obtained for the blue-shifted⁹ complex CIH \cdots FB, which is clearly a little fault of our calculation, as can be verified considering the negative estimate reported by McDowell and Buckingham.⁹

3.1 Topological analysis

In order to appreciate the contribution that different regions of the molecular space give to $\sigma_{\perp}^{\text{H}}$, the stagnation graph (SG)^{13,14} of $\mathbf{J}^{\mathbf{B}}$ induced by a static magnetic field perpendicular to the H-bond has been determined. The SG shows the lines and isolated singularities at which the current density vector field vanishes. These are interpreted via theoretical tools described elsewhere.^{16,17} Since, neglecting the vector component of $\mathbf{J}^{\mathbf{B}}$ parallel to \mathbf{B} has no consequence on the computed molecular magnetic properties, see later, the SG obtained using the two components of $\mathbf{J}^{\mathbf{B}}$ perpendicular to \mathbf{B} , hereafter referred to as pseudo-SG,³⁴ has been considered.

As can be expected for the summation of two distant diatropic vortices,³⁵ for all examined complexes, the pseudo-SG in the H-bond region is characterized by a continuous sequence of saddles, i.e., a continuous manifold of (2,0) points, which follows a path almost perpendicular to H \cdots Y and intersects the hydrogen bond very close to the H-bond critical point (BCP).^{36,37} Taking all the asymptotic trajectories originating and terminating at the saddle points along the stagnation line,

Table 1 B97-2/aug-cc-pVTZ optimized distances (in Å), relaxed interaction energies ΔE (in kJ mol⁻¹) and proton magnetic shielding components (in ppm)

Species	r_{X-H}	$r_{H...Y}$	Δr_{X-H}	ΔE	σ_{\perp}^H	σ_{\parallel}^H	σ_{iso}^H	$\Delta\sigma_{\perp}^H$	$\Delta\sigma_{\parallel}^H$	$\Delta\sigma_{iso}^H$
CIH	1.277				24.17	45.72	31.35			
CIH...FB	1.277	2.907	0.000	-0.2	23.61	47.25	31.49	-0.56	1.53	0.14
CIH...OC	1.277	2.630	0.001	-2.3	23.09	47.78	31.32	-1.08	2.05	-0.04
CIH...N ₂	1.278	2.559	0.001	-3.0	22.73	48.00	31.15	-1.44	2.27	-0.20
CIH...CO	1.282	2.421	0.005	-6.2	21.36	48.27	30.33	-2.81	2.55	-1.02
CIH...BF	1.296	2.271	0.019	-14.1	17.79	48.30	27.96	-6.38	2.58	-3.40
CIH...NCH	1.288	2.095	0.012	-15.5	18.45	49.21	28.70	-5.72	3.48	-2.65

two surfaces, hereafter called *separatrices* after Gomes,¹⁴ are found that provide a net separation of the current density in three spatial *domains of current*: a first one enclosing X–H (hereafter called \mathcal{H}), a second one enclosing Y–Z (hereafter called \mathcal{Y}), and a third external, delocalized one enclosing the former two (hereafter called \mathcal{E}); see Figure 1 for the CIH...BF case and the ESI for the full set of complexes.

As can be seen, current trajectories originate from and terminate at the same saddle point. In addition to the saddle line, Figure 1 shows also a line of centers (green dots) that merges with the line of saddles at about $6 a_0$ from the molecular axis. The current above this merging point belongs to the \mathcal{E} domain, as well as the current surrounding the domains \mathcal{H} and \mathcal{Y} .

Since the separatrices are formed by current trajectories infinitely close one to each other, each separatrix looks like a kind of impenetrable wall and no current perpendicular to \mathbf{B} can enter or leave the internal domain, which therefore is a *basin* of current confinement—not to be confused with the atomic basins of the QTAIM.³⁸ In other words, owing to the lack of any unphysical source or sink of current, an integral condition for the conservation of the current perpendicular to \mathbf{B} can be written for each domain as^{39,40}

$$\begin{aligned} \int_{\mathcal{D}} J_{\alpha}^{B\delta} d\mathbf{r} = 0 &\implies \int_{\mathcal{D}} \mathcal{J}_{\alpha}^{B\delta} B_{\delta} d\mathbf{r} = 0 \implies \\ &\implies \int_{\mathcal{D}} \mathcal{J}_{\alpha}^{B\delta} d\mathbf{r} = 0 \quad \alpha \neq \delta \end{aligned} \quad (4)$$

where $\int_{\mathcal{D}} \dots d\mathbf{r}$ means volume integration over domain \mathcal{D} and, according to a standard notation,⁴¹ $\mathcal{J}_{\alpha}^{B\delta} = \mathcal{J}_{\alpha}^{B\delta}(\mathbf{r})$ is the second rank current density tensor. Here and after tensor notation is employed, i.e., the Einstein convention of summing over repeated Greek indices is in force and $\varepsilon_{\alpha\beta\gamma}$ is the Levi-Civita third-rank pseudotensor.

Condition (4) can be used to define basin contributions to the diagonal components of the magnetizability tensor that are origin-independent. Briefly, assuming the supra-molecular axis aligned with the z Cartesian direction, and the two origins \mathbf{r}_0 and \mathbf{r}'_0 separated by the vector displacement \mathbf{d} , i.e.,

$\mathbf{r}'_0 = \mathbf{r}_0 + \mathbf{d}$, one has

$$\begin{aligned} \xi'_{xx,\mathcal{D}} &= \frac{1}{2} \varepsilon_{x\beta\gamma} \int_{\mathcal{D}} (r_{\beta} - r'_{0\beta}) \mathcal{J}_{\gamma}^{B_x} d\mathbf{r} = \\ &= \frac{1}{2} \varepsilon_{x\beta\gamma} \int_{\mathcal{D}} (r_{\beta} - r_{0\beta} - d_{\beta}) \mathcal{J}_{\gamma}^{B_x} d\mathbf{r} = \\ &= \frac{1}{2} \varepsilon_{x\beta\gamma} \int_{\mathcal{D}} (r_{\beta} - r_{0\beta}) \mathcal{J}_{\gamma}^{B_x} d\mathbf{r} = \xi_{xx,\mathcal{D}}, \end{aligned} \quad (5)$$

which proves the above assertion; a generalization can be easily worked out. As a major consequence, the perpendicular magnetizability ξ_{\perp} can be decomposed into origin-independent basin-contributions $\xi_{\perp,\mathcal{D}}$. The nuclear magnetic shielding does not depend on any origin and the partition of σ_{\perp}^H in basin contributions comes directly from the current confinement. Total components can be recovered as

$$\xi_{\perp} = \sum_{\mathcal{D}} \xi_{\perp,\mathcal{D}}, \quad (6)$$

$$\sigma_{\perp}^H = \sum_{\mathcal{D}} \sigma_{\perp,\mathcal{D}}^H. \quad (7)$$

In practical application eqn (4) is not exactly fulfilled. This has no consequence on calculated $\sigma_{\perp,\mathcal{D}}^H$, whilst it has some effect on $\xi_{\perp,\mathcal{D}}$ of polar systems only, which can be largely reduced using adequate basis sets.^{23–26} All the above demonstrates the possibility to decompose the magnetic properties in a rather natural way exploiting the topology of the induced current density field and offers a different point of view from that given by Bader and Keith with their method of the properties of atoms in molecules.⁴²

3.2 Decomposition of magnetic properties

Basin contributions to σ_{\perp}^H and ξ_{\perp} can be calculated carrying out separate volume integrations of the perpendicular proton magnetic shielding density function^{43,44} $\Sigma_{\perp}^H = \Sigma_{\perp}^H(\mathbf{r})$ and perpendicular magnetizability density function $\Xi_{\perp} = \Xi_{\perp}(\mathbf{r})$ respectively, one for each domain of current inside a separatrix. Since our main target here is the proton magnetic shielding, much of the following discussion will deal with such a

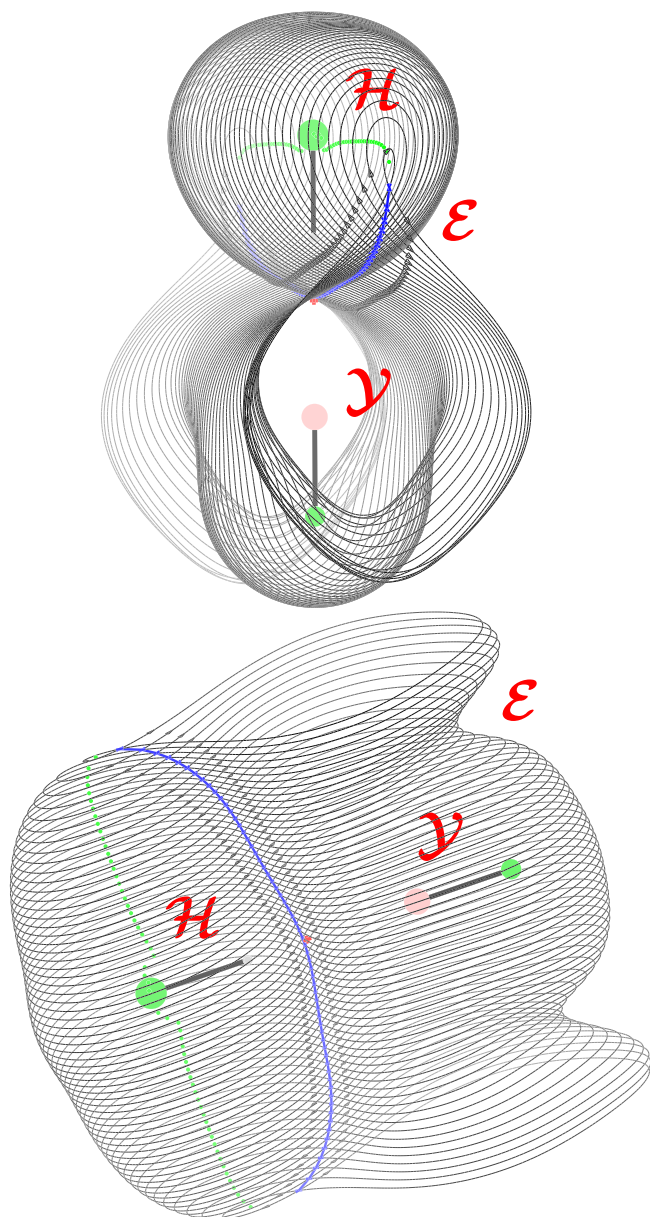


Fig. 1 Two different views of the separatrixes of the current density induced by a magnetic field perpendicular to the H-bond, calculated at B97-2/aug-cc-pVTZ level of theory using the CTOCD-DZ2 approach for the ClH...BF linear complex. Only asymptotic trajectories originating and terminating at saddle points $0.2 a_0$ far apart along the saddle line (in blue) are shown. The current density domains, or basins of current, enclosed within the separatrixes are indicated by the symbol \mathcal{H} and \mathcal{Y} , whilst \mathcal{E} indicates the external domain surrounding the former two. Fluorine and chlorine are green, boron is pink and hydrogen is light gray. A line of centers (small green dots) passing through chlorine is also reported. The BCP of the electron density is marked by a small red cross.

Table 2 Basin perpendicular magnetizabilities of ClH...BF computed for different choice of the origin (in au)

Origin	\mathcal{Y}	\mathcal{H}	\mathcal{E}	Total
Cl	-1.4600	-4.3722	-1.3991	-7.2313
H	-1.4478	-4.3863	-1.3987	-7.2328
B	-1.4265	-4.4104	-1.3981	-7.2349
F	-1.4146	-4.4242	-1.3979	-7.2367
average	-1.4372	-4.3983	-1.3985	-7.2339
std.dev.	0.02	0.02	0.001	0.002

Table 3 Decomposition of the perpendicular proton magnetic shielding into basin contributions (in ppm)

Species	$\sigma_{\perp, \mathcal{H}}^H$	$\sigma_{\perp, \mathcal{Y}}^H$	$\sigma_{\perp, \mathcal{E}}^H$	σ_{\perp}^H
ClH...FB	23.81	-0.44	0.23	23.60
ClH...OC	23.14	-0.46	0.40	23.08
ClH...N ₂	22.55	-0.40	0.57	22.72
ClH...CO	20.87	-0.33	0.82	21.35
ClH...BF	17.03	-0.36	1.12	17.78
ClH...NCH	18.07	-0.79	1.16	18.44

The computed σ_{\perp}^H values by means of eqn (7) reported in the last column show a small, irrelevant difference with respect to those in Table 1, due to the different method of integration.

quantity. However, the origin independence of the computed basin magnetizabilities, as required by eqn (5), is most important for the physical interpretation of the breakdown of the current density field. Therefore, an even brief assessment of such an origin independence is mandatory. Typical results are shown in Table 2, which collects the basin magnetizabilities of ClH...BF obtained integrating Ξ_{\perp} over domains \mathcal{Y} , \mathcal{H} and \mathcal{E} for some rather obvious different origins.

As can be observed, the degree of origin independence of the computed $\xi_{\perp, \mathcal{Y}}$ is rather good, as documented also by the very small standard deviations. Conversely, for an arbitrary dissection of the molecular space, the results are heavily origin-dependent. This can be best appreciated looking at the ESI for a couple of arbitrary partitions of the molecular space.

3.2.1 Proton magnetic shielding. Breakdown of the σ_{\perp}^H into basin contributions is shown in Table 3.

As can be observed, contributions from domains \mathcal{Y} and \mathcal{E} are relatively small and opposite in sign. The calculated $\sigma_{\perp, \mathcal{Y}}^H$ are fairly constant and show a deshielding effect of the base, which is, however, insufficient to account for the large decrease of σ_{\perp}^H on H-bond formation. Our results for $\sigma_{\perp, \mathcal{Y}}^H$ are consistent with the $\sigma_{xx}^{H(\text{mag})}$ computed by McDowell and Buckingham, who crudely supposed that the magnetic field at the position of the proton due to the magnetization of Y is that of the dipole generated by the magnetizability of Y.⁹ Conversely, the calculated $\sigma_{\perp, \mathcal{E}}^H$ increases the perpendicular proton magnetic shielding according to the trend: ClH...FB < ClH...OC

$\langle \text{CIH} \cdots \text{N}_2 \rangle < \langle \text{CIH} \cdots \text{CO} \rangle < \langle \text{CIH} \cdots \text{BF} \rangle < \langle \text{CIH} \cdots \text{NCH} \rangle$, which is the same trend, in terms of stability, of the relaxed interaction energies reported in Table 3. Interaction energies and $\sigma_{\perp, \mathcal{E}}^{\text{H}}$ values can be fitted with a linear relation (slope = -16.4 kJ/(mol ppm), $R^2=0.94$) that is particularly interesting if compared with the findings by Fliegl et al.¹² The H-bond current susceptibility (or current strength)^{45,46} reported by Fliegl et al.¹² corresponds to the strength of the current flowing in domain \mathcal{E} . Then, the larger the H-bond current susceptibility, the larger the contribution to the proton shielding, the larger the H-bond strength, in a rather nice synchronicity. As a result, the sum of the two contributions from domains \mathcal{Y} and \mathcal{E} tends to increase passing from a small proton deshielding for the less stable complexes to a net proton shielding for the more stable ones. Therefore, it emerges clearly that the large proton deshielding caused by the hydrogen bond formation is mainly a local effect, strictly confined within domain \mathcal{H} . This implies a non negligible variation of $\Sigma_{\perp}^{\text{H}}$, especially close to the hydrogen nucleus, that seems in contrast with some of the ideas developed so far modeling weak interactions, in particular with that of the promolecule model.⁴⁷

As a matter of fact, we remark that the shielding caused by the sum of the local current within domains \mathcal{Y} and the delocalized current in domain \mathcal{E} , which is opposite to the experimental trend, would be not quantifiable without the topological definition of the basins of current represented in Figure 1.

3.3 Density differences

According to the promolecule model, the main features of the supramolecular electron densities can be explained overlapping the electron densities of the non-interacting subunits.⁴⁷ It is not obvious to what extent this argument can be extended to other property densities. Then, to better understand why the model does not seem to work here for the perpendicular proton magnetic shielding density function and to gain a deeper insight, we have computed and visualized the difference

$$\Delta \Sigma_{\perp, \text{pro}}^{\text{H}} = \Sigma_{\perp}^{\text{H}}(\text{XH} \cdots \text{YZ}) - \Sigma_{\perp}^{\text{H}}(\text{promolecule}), \quad (8)$$

where $\Sigma_{\perp}^{\text{H}}(\text{XH} \cdots \text{YZ})$ is the perpendicular proton magnetic shielding density function of the complexes and $\Sigma_{\perp}^{\text{H}}(\text{promolecule})$ is the sum of the perpendicular magnetic shielding density functions at the proton position of the two isolated, non-relaxed monomers, i.e., with exactly the same bond lengths they have in the complexes. Figure 2 shows a representative map of $\Delta \Sigma_{\perp, \text{pro}}^{\text{H}}$ calculated for the $\text{CIH} \cdots \text{BF}$ complex on a plane containing the supra-molecular axis. Similar plots have been obtained for all the complexes and are reported in the ESI. Actually, a large decrease of $\Sigma_{\perp}^{\text{H}}$ on H-bond formation can be observed, fully localized within domain \mathcal{H} in agreement to what expected on the basis of the previous topological analysis. The drop is essentially restricted around

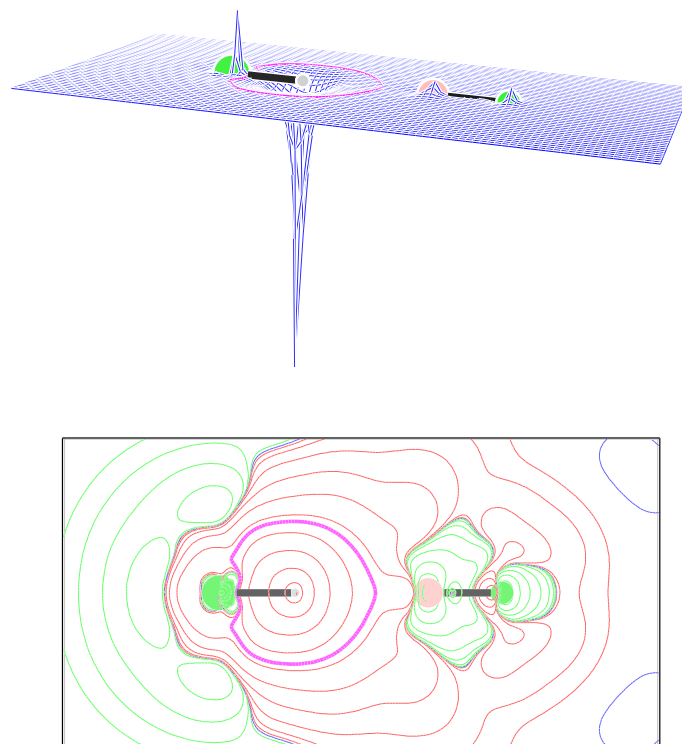


Fig. 2 The change in the perpendicular component of the proton shielding density arising from H-bond formation $\Delta \Sigma_{\perp, \text{pro}}^{\text{H}}$ for the $\text{CIH} \cdots \text{BF}$ complex on a plane containing the supra-molecular axis, see text for definitions. Negative/positive contours are red/green, scaled by 4. Minimum value that can be appreciated is -10 ppm/ a_0^3 . Magenta contour corresponds to -0.017 ppm/ a_0^3 .

Table 4 Breakdown of the perpendicular proton magnetic shielding change (in ppm) and local contributions, see text for definitions (Δn_{loc} is in e unit)

Species	$\Delta\sigma_{\perp,\text{geo}}^{\text{H}}$	$\Delta\sigma_{\perp,\text{YZ}'}^{\text{H}}$	$\Delta\sigma_{\perp,\text{pro}}^{\text{H}}$	$\Delta\sigma_{\perp,\text{loc}}^{\text{H}}$	Δn_{loc}
ClH...FB	-0.00	-0.48	-0.08	-0.10	-0.000
ClH...OC	-0.01	-0.57	-0.50	-0.52	-0.004
ClH...N ₂	-0.02	-0.55	-0.87	-0.87	-0.006
ClH...CO	-0.09	-0.58	-2.14	-2.01	-0.010
ClH...BF	-0.32	-0.64	-5.42	-4.93	-0.021
ClH...NCH	-0.20	-1.10	-4.42	-4.49	-0.028

the hydrogen atom, where $\Delta\sigma_{\perp,\text{pro}}^{\text{H}}$ shows a rather deep negative cone centered almost exactly on the hydrogen atom itself. The magenta contour in the figure approximates the zero-level leaving the chlorine atom on the outside. Upon moving to planes above (and below) the molecular plane, the shape of $\Delta\sigma_{\perp,\text{pro}}^{\text{H}}$ remains almost the same, while its magnitude goes quickly to zero within $2 a_0$ for all the complexes here examined.

Integrating eqn (8) all over the molecular space one has

$$\Delta\sigma_{\perp,\text{pro}}^{\text{H}} = \sigma_{\perp}^{\text{H}} - \left(\sigma_{\perp,\text{XH}'}^{\text{H}} + \Delta\sigma_{\perp,\text{YZ}'}^{\text{H}} \right), \quad (9)$$

where the ‘‘prime’’ indicates the non relaxed monomers. Then, from the definition

$$\Delta\sigma_{\perp,\text{geo}}^{\text{H}} = \sigma_{\perp,\text{XH}'}^{\text{H}} - \sigma_{\perp,\text{XH}}^{\text{H}} \quad (10)$$

and using eqn (1) one obtains

$$\Delta\sigma_{\perp,\text{pro}}^{\text{H}} = \Delta\sigma_{\perp}^{\text{H}} - \Delta\sigma_{\perp,\text{geo}}^{\text{H}} - \Delta\sigma_{\perp,\text{YZ}'}^{\text{H}}, \quad (11)$$

where $\Delta\sigma_{\perp,\text{geo}}^{\text{H}}$ is the change in the perpendicular proton magnetic shielding of isolated ClH due to the bond length variation from relaxed to non-relaxed molecule, and $\Delta\sigma_{\perp,\text{YZ}'}^{\text{H}}$ is the contribution to the perpendicular proton magnetic shielding due to the isolated non-relaxed base. These can be easily evaluated and are reported in second and third columns of Table 4. As can be observed, both terms provide a proton deshielding; however, the Cl–H bond variation gives an almost negligible effect, whilst the base contribution provides only a fraction of the whole effect, in agreement with the $\sigma_{\perp,\text{YZ}'}^{\text{H}}$ values in Table 3 despite the much larger integration domain. The failure of the promolecule model can now be quantified by means of eqn (11). Results are given in the fourth column of Table 4 and, clearly, the greater the H-bond strength the larger is the deviation, which tends to account for the proton deshielding almost exclusively.

Owing to the $1/r^2$ scaling factor^{43,44} of the shielding density function, such a behavior is compatible with a decrease in current density strength around the hydrogen nucleus, which can be related, in first approximation, to a decrease of the

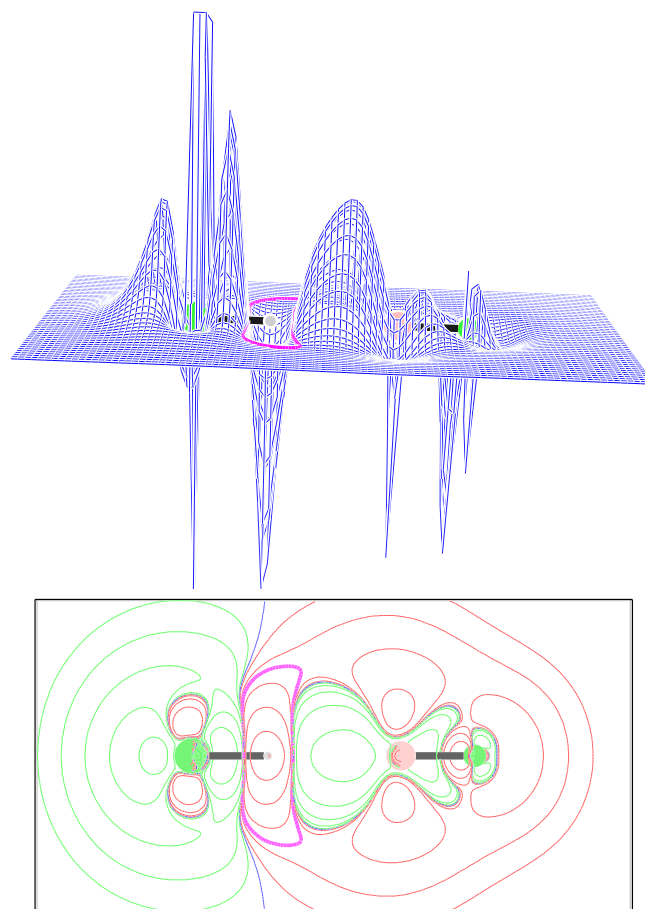


Fig. 3 The change in the charge density function arising from H-bond formation $\Delta\rho_{\text{pro}}$ for the ClH...BF complex on a plane containing the supra-molecular axis. Negative/positive contours are red/green, scaled by 4. Minimum value that can be appreciated is $-0.01 e/a_0^3$. Magenta contour corresponds to $-0.7 \times 10^{-4} e/a_0^3$.

charge density function $\rho = \rho(\mathbf{r})$ on the basis of the classic formula $\mathbf{J} = \rho\mathbf{v}$. In order to see that, we have evaluated the quantity

$$\Delta\rho_{\text{pro}} = \Delta\rho - \Delta\rho_{\text{geo}} - \Delta\rho_{\text{YZ}'} \quad (12)$$

which is the analogous of eqn (11) for the charge density function. Figure 3 shows a map $\Delta\rho_{\text{pro}}$ for the $\text{CIH}\cdots\text{BF}$ complex, see the ESI for the other complexes. Indeed, upon H-bond formation, a drop of the charge density centered almost exactly on the hydrogen nucleus can be observed, which ultimately furnishes the rationalization searched for.

In order to appreciate the local or non-local character of the deshielding effect, we have also evaluated the integral of $\Delta\Sigma_{\perp,\text{pro}}^{\text{H}}$ inside a volume determined by stacking near-zero-value contours (magenta in fig. 2) from $2a_0$ above to $-2a_0$ below the supra-molecular plane. The result is reported in Table 4 under the heading $\Delta\sigma_{\perp,\text{loc}}^{\text{H}}$. As can be observed, the latter is always very close to $\Delta\sigma_{\perp,\text{pro}}^{\text{H}}$, indicating a very local nature of the deshielding effect. The integration of $\Delta\rho_{\text{pro}}$ within the analogous near-zero-value contours (magenta in fig. 3) gives the loss of electron Δn_{loc} in the neighborhood of the hydrogen reported in the last column of Table 4. Eventually, it can be appreciated that a drop as small as 2–3% of an electron produces a proton NMR deshielding as big as 4.5–5 ppm. This makes the NMR detection of H-bond formation a very sensible technique.

4 Conclusions

In conclusion, if, on the one hand, $\sigma_{\parallel}^{\text{H}}$ is basically understood to be increased on H-bond formation by a magnetic effect due to induced diatropic circulations distributed all along $\text{X-H}\cdots\text{Y}$ portion of the complex, on the other hand, $\sigma_{\perp}^{\text{H}}$ is now assessed, on the basis of the results here presented, to be largely decreased as a consequence of a local loss of electronic charge density on the hydrogen in the $\text{X-H}\cdots\text{Y}$. The electron depletion on hydrogen, not larger than 3% of an electron for the complexes studied here, but likely larger for more tightly hydrogen bonded systems, triggers a local reduction of the current density that in turn, owing to the $1/r^2$ scaling factor of the shielding density, produces the final large deshielding effect. The local nature of the effect appears clearly from the confinement of the current density induced by a magnetic field perpendicular to the H-bond, as imposed by the presence of a (pseudo) stagnation line of (2,0) saddle points, which is suggested to be a common feature of most hydrogen bonded systems, like the presence of a BCP already accounted in the theoretical criterion C6 and footnote F9 of the IUPAC 2011 recommendations.²

Acknowledgement

Financial support from the MIUR and Università di Salerno is gratefully acknowledged.

References

- 1 E. Arunan, G. R. Desiraju, R. A. Klein, J. Sadlej, S. Scheiner, I. Alkorta, D. C. Clary, R. H. Crabtree, J. J. Dannenberg, P. Hobza, H. G. Kjaergaard, A. C. Legon, B. Mennucci and D. J. Nesbitt, *Pure Appl. Chem.*, 2011, **83**, 1619–1636.
- 2 E. Arunan, G. R. Desiraju, R. A. Klein, J. Sadlej, S. Scheiner, I. Alkorta, D. C. Clary, R. H. Crabtree, J. J. Dannenberg, P. Hobza, H. G. Kjaergaard, A. C. Legon, B. Mennucci and D. J. Nesbitt, *Pure Appl. Chem.*, 2011, **83**, 1637–1641.
- 3 G. R. Desiraju, *Angew. Chem., Int. Ed.*, 2011, **50**, 52–59.
- 4 *IUPAC Compendium of Chemical Terminology*, Royal Society of Chemistry, Cambridge, UK, the online version mostly corresponds to second edn, 1997.
- 5 F. Weinhold and R. A. Klein, *Mol. Phys.*, 2012, **110**, 565–579.
- 6 J. R. Lane, J. Contreras-García, J.-P. Piquemal, B. J. Miller and H. G. Kjaergaard, *J. Chem. Theory Comput.*, 2013, **9**, 3263–3266.
- 7 G. A. Kumar and M. A. McAllister, *J. Org. Chem.*, 1998, **63**, 6968–6972.
- 8 J. E. Del Bene, S. A. Perera and R. J. Bartlett, *J. Phys. Chem. A*, 1999, **103**, 8121–8124.
- 9 S. A. C. McDowell and A. D. Buckingham, *Mol. Phys.*, 2006, **104**, 2527–2531.
- 10 M. Pecul, J. Leszczynski and J. Sadlej, *J. Chem. Phys.*, 2000, **112**, 7930.
- 11 M. Ferraro, P. Lazzeretti, R. Viglione and R. Zanasi, *Chem. Phys. Lett.*, 2004, **390**, 268–271.
- 12 H. Fliegl, O. Lehtonen, D. Sundholm and V. R. I. Kaila, *Phys. Chem. Chem. Phys.*, 2011, **13**, 434.
- 13 J. A. N. F. Gomes, *J. Chem. Phys.*, 1983, **78**, 4585.
- 14 J. A. N. F. Gomes, *Phys. Rev. A: At., Mol., Opt. Phys.*, 1983, **28**, 559–566.
- 15 T. A. Keith and R. F. W. Bader, *J. Chem. Phys.*, 1993, **99**, 3669.
- 16 S. Pelloni, F. Faglioni, R. Zanasi and P. Lazzeretti, *Phys. Rev. A: At., Mol., Opt. Phys.*, 2006, **74**, 012506.
- 17 S. Pelloni, P. Lazzeretti and R. Zanasi, *Theor. Chem. Acc.*, 2009, **123**, 353–364.
- 18 M. J. Frisch, G. W. Trucks, H. B. Schlegel, G. E. Scuseria, M. A. Robb, J. R. Cheeseman, G. Scalmani, V. Barone, B. Mennucci, G. A. Petersson, H. Nakatsuji, M. Caricato, X. Li, H. P. Hratchian, A. F. Izmaylov, J. Bloino, G. Zheng, J. L. Sonnenberg, M. Hada, M. Ehara, K. Toyota, R. Fukuda, J. Hasegawa, M. Ishida, T. Nakajima, Y. Honda, O. Kitao, H. Nakai, T. Vreven, J. A. Montgomery Jr., J. E. Peralta, F. Ogliaro, M. Bearpark, J. J. Heyd, E. Brothers, K. N. Kudin, V. N. Staroverov, T. Keith, R. Kobayashi, J. Normand, K. Raghavachari, A. Rendell, J. C. Burant, S. S. Iyengar, J. Tomasi, M. Cossi, N. Rega, J. M. Millam, M. Klene, J. E. Knox, J. B. Cross, V. Bakken, C. Adamo, J. Jaramillo, R. Gomperts, R. E. Stratmann, O. Yazyev, A. J. Austin, R. Cammi, C. Pomelli, J. W. Ochterski, R. L. Martin, K. Morokuma, V. G. Zakrzewski, G. A. Voth, P. Salvador, J. J. Dannenberg, S. Dapprich, A. D. Daniels, O. Farkas, J. B. Foresman, J. V. Ortiz, J. Cioslowski and D. J. Fox, *Gaussian 09, Revision D.01*, Gaussian, Inc., Wallingford CT, 2013.
- 19 P. J. Wilson, T. J. Bradley and D. J. Tozer, *J. Chem. Phys.*, 2001, **115**, 9233.
- 20 T. H. Dunning, *J. Chem. Phys.*, 1989, **90**, 1007.
- 21 D. E. Woon and T. H. Dunning, *J. Chem. Phys.*, 1993, **98**, 1358.
- 22 T. A. Keith and R. F. Bader, *Chem. Phys. Lett.*, 1993, **210**, 223–231.
- 23 P. Lazzeretti, M. Malagoli and R. Zanasi, *Chem. Phys. Lett.*, 1994, **220**, 299–304.
- 24 S. Coriani, P. Lazzeretti, M. Malagoli and R. Zanasi, *Theor. Chim. Acta*, 1994, **89**, 181–192.

- 25 R. Zanasi, P. Lazzeretti, M. Malagoli and F. Piccinini, *J. Chem. Phys.*, 1995, **102**, 7150.
- 26 R. Zanasi, *J. Chem. Phys.*, 1996, **105**, 1460.
- 27 R. W. Havenith and P. W. Fowler, *Chem. Phys. Lett.*, 2007, **449**, 347–353.
- 28 A. Soncini, A. M. Teale, T. Helgaker, F. De Proft and D. J. Tozer, *J. Chem. Phys.*, 2008, **129**, 074101.
- 29 R. W. Havenith, A. J. Meijer, B. J. Irving and P. W. Fowler, *Mol. Phys.*, 2009, **107**, 2591–2600.
- 30 P. Lazzeretti, M. Malagoli and R. Zanasi, *Technical Report on Project "Sistemi Informatici e Calcolo Parallelo"*, CNR Research Report I/67, 1991.
- 31 P. W. Fowler, E. Steiner, R. W. A. Havenith and L. W. Jenneskens, *Magn. Reson. Chem.*, 2004, **42**, S68–S78.
- 32 D. Flaig, M. Maurer, M. Hanni, K. Braunger, L. Kick, M. Thubauville and C. Ochsenfeld, *J. Chem. Theory Comput.*, 2014, **10**, 572–578.
- 33 J. J. Novoa and C. Sosa, *J. Phys. Chem.*, 1995, **99**, 15837–15845.
- 34 R. Carion, B. Champagne, G. Monaco, R. Zanasi, S. Pelloni and P. Lazzeretti, *J. Chem. Theory Comput.*, 2010, **6**, 2002–2018.
- 35 G. Monaco and R. Zanasi, *J. Chem. Phys.*, 2009, **131**, 044126.
- 36 P. L. A. Popelier and R. F. W. Bader, *J. Phys. Chem.*, 1994, **98**, 4473–4481.
- 37 U. Koch and P. L. A. Popelier, *J. Phys. Chem.*, 1995, **99**, 9747–9754.
- 38 R. F. W. Bader, *Atoms in molecules: a quantum theory*, Clarendon Press ; Oxford University Press, Oxford [England] : New York, 1994.
- 39 S. T. Epstein, *J. Chem. Phys.*, 1973, **58**, 1592.
- 40 H. Sambe, *J. Chem. Phys.*, 1973, **59**, 555.
- 41 P. Lazzeretti, *Prog. Nucl. Magn. Reson. Spectrosc.*, 2000, **36**, 1–88.
- 42 R. F. W. Bader and T. A. Keith, *J. Chem. Phys.*, 1993, **99**, 3683.
- 43 C. J. Jameson and A. D. Buckingham, *J. Phys. Chem.*, 1979, **83**, 3366–3371.
- 44 C. J. Jameson and A. D. Buckingham, *J. Chem. Phys.*, 1980, **73**, 5684.
- 45 J. Jusélius, D. Sundholm and J. Gauss, *J. Chem. Phys.*, 2004, **121**, 3952.
- 46 H. Fliegl, S. Taubert, O. Lehtonen and D. Sundholm, *Phys. Chem. Chem. Phys.*, 2011, **13**, 20500.
- 47 M. A. Spackman, *Chem. Phys. Lett.*, 1999, **301**, 425–429.